

Nuclear Physics with Chiral Effective Field Theory: State of the Art and Open Challenges

Evgeny Epelbaum^{*†}

Institut für Theoretische Physik II, Ruhr-Universität Bochum, D-44780 Bochum, Germany

E-mail: evgeny.epelbaum@rub.de

Understanding the properties of atomic nuclei and nuclear dynamics from QCD remains a major challenge. Complementary to first attempts along these lines based on lattice QCD, an effective field theory approach has been developed in the past two decades and applied to a variety of nuclear bound states and reactions. I outline the foundations of this method, review selected applications and address some open challenges in this field.

*Xth Quark Confinement and the Hadron Spectrum,
October 8-12, 2012
TUM Campus Garching, Munich, Germany*

^{*}Speaker.

[†]It is a great pleasure to thank all my collaborators for sharing their insights into the discussed topics and the organizers of Confinement X for making this exciting conference possible. I also thank Ashot Gasparyan, Jambul Gegelia, Hermann Krebs, Timo Lähde, Deen Lee and Ulf-G. Meißner for reading the manuscript and making many valuable suggestions. Finally, I acknowledge financial support by the European Research Council (ERC-2010-StG 259218 NuclearEFT) and the Deutsche Forschungsgemeinschaft (SFB/TR 16).

1. Introduction

The past decade has witnessed a renewed interest in the nuclear force problem. In addition to new experimental facilities, this is to a large extent related to exciting theoretical developments in this field. On the one hand, rapidly increasing computational resources and improvements in algorithms make some nuclear physics observables amenable to numerical simulations in lattice QCD [1]. Complementary to this research direction, considerable progress has been achieved towards a quantitative description of nuclear forces and dynamics within the framework of effective field theory (EFT) starting from the pioneering work of Weinberg [2]. The essential idea behind this method is to systematically exploit the scale separation in a problem of interest. There are several scales that play an important role in nuclear physics. The lowest one is given by the typical binding energies of the order of a few MeV per nucleon. This small scale manifests itself in the large values of the nucleon-nucleon (NN) S-wave scattering lengths, $a_{1S0} \sim (8 \text{ MeV})^{-1}$ and $a_{3S1} \sim (40 \text{ MeV})^{-1}$, and signals the breakdown of perturbation theory for two- and many-nucleon observables at low energy. It is well separated from the next-higher scale relevant for the NN system, namely the pion mass M_π . Exploiting this scale separation allows one to set up the so-called pionless EFT. In this approach, (non-relativistic) nucleons are treated as the only active degrees of freedom (DOFs) and the shallow scale associated with the nuclear binding is generated dynamically via resumming the lowest-order NN interactions. Pionless EFT is justified for momenta well below M_π which is sufficient for e.g. many reactions of astrophysical interest. Similar theoretical methods are successfully applied to study Efimov physics and universality in few-body systems close to the unitary limit, cold atoms and the properties of halo-nuclei, see e.g. [3] for a recent review article.

To increase the applicability range of the theory beyond the near-threshold region one needs to include pions as explicit DOFs. The resulting chiral EFT (χ EFT) relies on the approximate spontaneously broken chiral symmetry of QCD. This symmetry/symmetry-breaking pattern of QCD strongly constrains the interactions of pions being identified with the corresponding pseudo-Goldstone bosons. It allows one to calculate pion and pion-nucleon low-energy observables within a systematic perturbative expansion in Q/Λ_χ . Here, $Q \sim M_\pi$ refers to the soft scale associated with external momenta while $\Lambda_\chi \sim M_\rho$ GeV stands for the (hard) chiral-symmetry breaking scale that governs the values of renormalized low-energy constants (LECs) in the effective Lagrangian. We refer the reader to the review article [4] and references therein for more details on chiral perturbation theory (ChPT) and an overview of recent trends and developments in that field.

In the past decades, χ EFT has been extensively applied to the nuclear force problem, see [5] for an introduction and [6, 7] for recent review articles. In this framework, nucleons interact by exchanging a single or multiple pions. In the chiral limit of vanishing quark masses one is expanding about, these interactions have an infinitely long range. The long-range tail of the nuclear force controls the energy dependence of the scattering amplitude. It is strongly constrained by the chiral symmetry of QCD and can be rigorously derived in ChPT, see Fig. 1. On the other hand, the short-range part of the range well below M_π^{-1} is driven by physics that cannot be resolved explicitly in reactions with typical nucleon momenta of $\mathcal{O}(M_\pi)$. Such short-range forces can be naturally parameterized by contact interactions with an increasing number of derivatives.

In this contribution I review the current status of χ EFT for nuclear forces and few-nuclear systems, discuss some recent and ongoing developments and address open questions and challenges

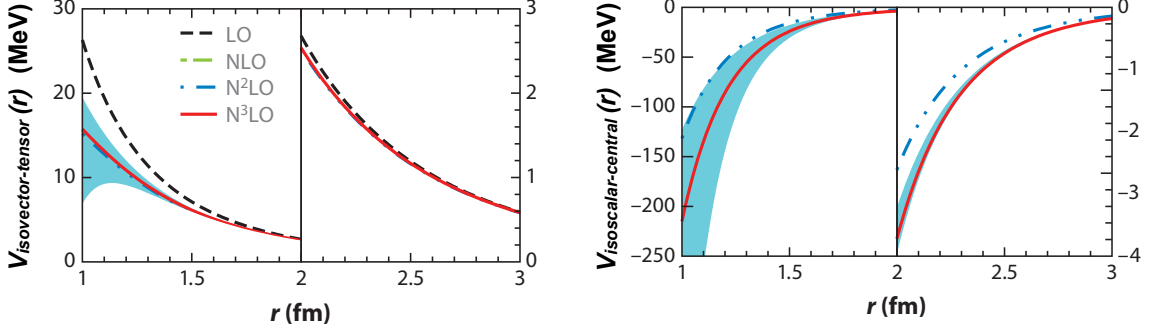


Figure 1: Chiral expansion of the isovector-tensor (left panel) and isoscalar central (right panel) long-range two-nucleon potentials. The shaded bands show an estimated size of (scheme-dependent) short-range contributions which are represented by contact interactions, see Ref. [5] for more details.

in this field. The paper is organized as follows. Section 2 is devoted to nuclear forces and nuclear chiral dynamics. A few recent applications to few-nucleon reactions with external probes are discussed in section 3. Finally, section 4 overviews progress towards understanding the properties of light nuclei via lattice simulations of χ EFT.

2. Chiral effective field theory for nuclear forces and light nuclei

Assuming that LECs accompanying few-nucleon contact interactions scale according to naive dimensional analysis, the chiral power counting provides a natural qualitative explanation of the (always assumed) dominance of the two-body interactions with $\langle V_{2N} \rangle \gg \langle V_{3N} \rangle \gg \langle V_{4N} \rangle \gg \dots$. More precisely, the chiral expansion of nuclear forces has the form [2]

$$\begin{aligned}
 V_{2N} &= V_{2N}^{(0)} + V_{2N}^{(2)} + V_{2N}^{(3)} + V_{2N}^{(4)} + \dots, \\
 V_{3N} &= V_{3N}^{(3)} + V_{3N}^{(4)} + \dots, \\
 V_{4N} &= V_{4N}^{(4)} + \dots,
 \end{aligned} \tag{2.1}$$

where the superscripts denote the associated powers of the soft scale Q .

2.1 The two-nucleon system

Starting from the pioneering work by Weinberg [2] and the first quantitative calculation of Ref. [8], the NN force has been extensively studied in the framework of χ EFT. Within the heavy-baryon formulation, calculations have been pushed to leading two-loop order corresponding to next-to-next-to-next-to-leading order (N^3 LO) or Q^4 in the chiral expansion. At this order, the long-range part of the NN force is governed by exchange of up to three pions. It is strongly constrained by the chiral symmetry of QCD and experimental data on pion-nucleon scattering. The short-range part depends on 26 LECs accompanying 24 isospin-invariant and 2 isospin-breaking NN contact interactions which are tuned to the low-energy NN data [9, 10]. It was found to be necessary and sufficient to go to N^3 LO in order to accurately describe NN phase shifts up to energies of the order of $E_{\text{lab}} \sim 200$ MeV.

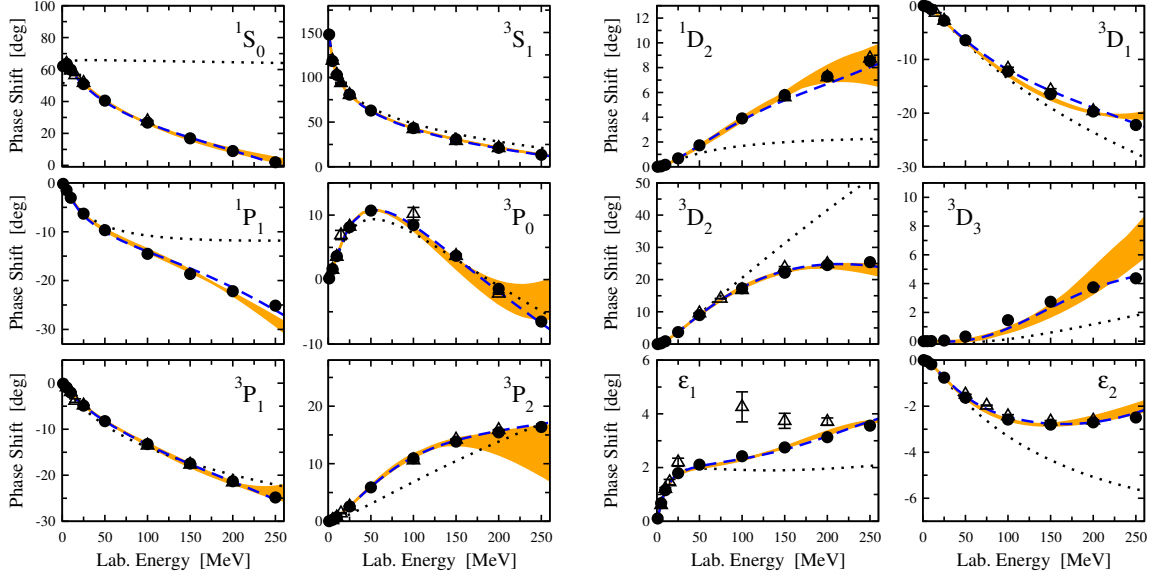


Figure 2: Neutron-proton phase shifts and mixing angles calculated using $N^3\text{LO}$ χEFT potentials of Ref. [10] (shaded bands) and Ref. [9] (dashed lines) in comparison with the Nijmegen [11] (filled circles) and SAID [12] (open triangles) partial wave analyses. Also shown are leading-order cutoff-independent results of Ref. [13] (dotted lines).

The most interesting part of the novel chiral NN force is two-pion (2π -) exchange which constitutes the second-longest contribution to the NN potential and, therefore, has significant impact on the energy dependence of the scattering amplitude. Indeed, its evidence has been confirmed in the partial wave analysis of the Nijmegen group [14], see also [15]. In agreement with expectations based on phenomenological studies, one observes a very strong attractive isoscalar central potential. This by far the strongest 2π -exchange contribution emerges, however, only at next-to-next-to-leading order ($N^2\text{LO}$) as a correction to the nominally dominant 2π -exchange potential at next-to-leading order (NLO). This peculiar pattern is well understood and can be traced back to the intermediate excitation of the $\Delta(1232)$ isobar at one of the nucleons which gives rise to a very strong attractive isoscalar central NN force [8, 16, 17]. In the standard formulation of χEFT based on pions and nucleons as the only explicit DOFs, all effects of the Δ (and heavier resonances as well as heavy mesons) are hidden in the (renormalized) values of (some of the) LECs starting from the subleading effective Lagrangian. As a consequence, the phenomenologically important 2π -exchange mechanism driven by the Δ excitation appears only at subleading order from diagrams involving one insertion of the subleading pion-nucleon vertex. The values of the corresponding LECs $c_{3,4}$ are, to a large extent, driven by the Δ isobar [18] and turn out to be rather large in magnitude. It is possible to improve the convergence of the EFT expansion by treating the Δ -isobar as an explicit DOF in the effective Lagrangian and counting $m_\Delta - m_N \sim M_\pi = \mathcal{O}(Q)$ [19], see also [20] for an alternative counting scheme. In such a Δ -full theory, the major part of the strong attractive 2π -exchange potential is shifted from $N^2\text{LO}$ to NLO, while the LECs $c_{3,4}$ take more natural values [17].

Having developed χEFT for the NN system, it is natural to address the question of the light quark-mass- (m_q -) dependence of the nuclear force and observables such as e.g. the deuteron bind-

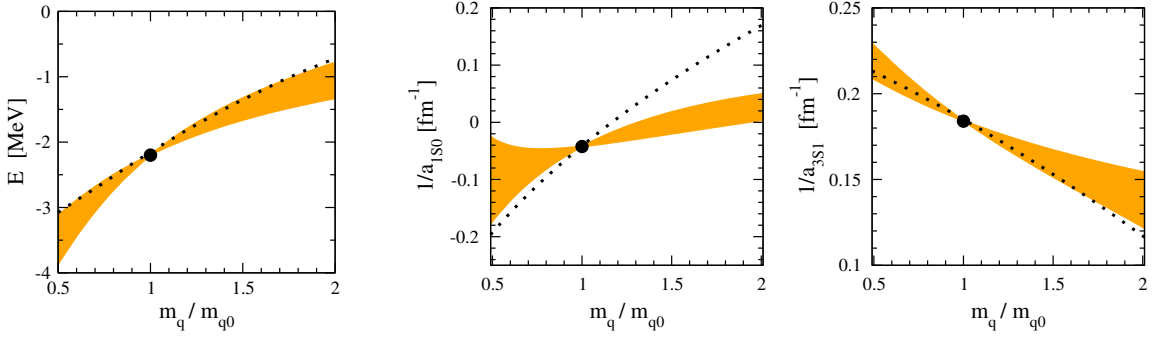


Figure 3: Quark mass dependence of the deuteron binding energy (left panel), and inverse $^1S_0/{}^3S_1$ neutron-proton scattering lengths (middle/right panel). Shaded bands correspond to the N^2 LO analysis of Ref. [28] as explained in the text. Also shown are leading-order cutoff-independent results of Refs. [13, 29].

ing energy E_{2H} and S-wave scattering lengths a_{1S0} , a_{3S1} . This is not only of considerable interest for ongoing and upcoming lattice-QCD calculations, but also for searches of a possible spatial and temporal variation of fundamental constants in nature [21] and questions related to anthropic considerations, see also section 4. The m_q -dependence of NN S-wave phase shifts and E_{2H} was analyzed at NLO in Ref. [22], see also Ref. [23] for a calculation using the power counting scheme of Ref. [24], which relies on a perturbative treatment of 1π -exchange, and more recent related studies [25, 26]. The common problem in all these calculations is the lack of knowledge about the m_q -dependence of NN contact interactions. Estimating the size of the corresponding LECs by means of dimensional analysis leads to a very large uncertainty for chiral extrapolations of E_{2H} , a_{1S0} and a_{3S1} . In addition, there are indications that the chiral expansion of the short-range part of the NN force might converge slowly in the heavy-baryon approach due to the appearance of the momentum scale $\sqrt{M_\pi m_N}$ associated with radiative pions [27]. To overcome these difficulties, the recent N^2 LO analysis of Ref. [28] made use of the fact that the LECs accompanying NN contact interactions are saturated by heavy-meson exchanges [30, 31]. Using a unitarized version of ChPT in combination with lattice-QCD results to describe the m_q -dependence of meson resonances saturating these LECs, the m_q -dependence of NN observables was analyzed at N^2 LO without relying on the chiral expansion of the short-range NN force, see Fig. 3. This allowed us to considerably reduce the theoretical uncertainty as compared to the earlier calculations. Extending these results to light nuclei and comparing observed and calculated primordial deuterium and helium abundances yields a stringent limit on a variation of the light quark mass, $\delta m_q / m_q = 0.2 \pm 0.04$, see also the related earlier calculation in Ref. [21]. While the calculated chiral extrapolations for E_{2H} are consistent with our earlier analysis in [22] as well as with the recent phenomenological calculation of Ref. [32], unquenched lattice-QCD results of the NPLQCD Collaboration [33] seem to indicate an opposite trend with a stronger-bound deuteron at large values of m_q . It is not clear at this stage whether there is any contradiction since the lattice results are so far only available at rather large pion masses with $M_\pi > 353.7$ MeV, see [1]. Using the available lattice data in conjunction with the (presumably unrealistic) assumptions of (i) perturbativeness of the 1π -exchange potential in the 3S_1 - 3D_1 channel and (ii) validity of the chiral expansion for NN scattering at such large values of M_π leads to a qualitatively different dependence of E_{2H} on m_q [25, 26].

Complementary to the studies based entirely on χ EFT, there are interesting recent developments towards merging χ EFT with dispersion relations [34, 35]. The main idea of this approach is to take advantage of the known analytic structure of the NN scattering amplitude $T(s)$, with s being the invariant mass of the NN system, which can be reconstructed from the so-called generalized potential $U(s)$ by means of the (once subtracted) dispersion relation

$$T(s) = U(s) + \int_{4m_N^2}^{\infty} \frac{ds'}{\pi} \frac{s - \mu_M^2}{s' - \mu_M^2} \frac{T(s)\rho(s')T^*(s')}{s' - s - i\epsilon}, \quad (2.2)$$

where $\rho(s)$ is the phase-space function (see Ref. [35] for the exact definition). Further, μ_M denotes the matching point for which $T(\mu_M) = U(\mu_M)$. The generalized potential does not have the right-hand elastic unitarity cut but still features left-hand cuts associated with t -channel pion exchanges and short-range mechanisms. The discontinuity across the first left-hand cut is unambiguously given by the 1π -exchange potential. The discontinuity across the left-hand cut in the range from $s = 4m_N^2 - 4M_\pi^2$ to $s = 4m_N^2 - 9M_\pi^2$ is calculated in Ref. [35] at N²LO using a manifestly covariant version of ChPT. This relies on the assumption of the validity of ChPT for the NN amplitude in some region below threshold. Extrapolating the contributions from more distant left-hand cuts in $U(s)$ to the physical region by means of a suitable conformal mapping [36, 37] or, more precisely, the Taylor expansion in a conformal variable $\xi(s)$, we solved in Ref. [35] the partial-wave projected nonlinear equation (2.2) for $T(s)$ using the N/D method. Fixing the constants entering the expansion in $\xi(s)$ of the short-range part of $U(s)$ in S - and P -waves from NN phase shifts up to the energy of $E_{\text{lab}} = 100$ MeV, the energy dependence could be reasonably well described up to $E_{\text{lab}} = 250$ MeV. We also observed good convergence of the chiral expansion for $U(s)$ when going from the order Q^0 to Q^3 (which supports the assumption about perturbativeness of the amplitude below threshold) and clear evidence for the 1π - and 2π -exchange cuts in NN phase shifts.

2.2 The three-nucleon force

Three-nucleon forces (3NF) represent an old but still very current topic in nuclear physics, see Refs. [38, 39] for recent review articles. While effects of 3NFs in low-energy nuclear observables are expected to be considerably smaller than the ones of the NN force, see Eq. (2.1), their inclusion is necessary at the level of accuracy of today's few- and many-body *ab-initio* calculations, see [38, 39] and references therein. In spite of decades of effort, the structure of the 3NF is not properly described by the available phenomenological models [38]. Given the very rich spin-momentum structure of the 3NF, scarcer database for nucleon-deuteron (Nd) scattering compared to the NN system and relatively high computational cost of solving the Faddeev equations, further progress in this fields requires substantial input from theory. This provides a strong motivation to study the 3NF within χ EFT.

The first nonvanishing contributions to the 3NF emerge at N²LO from tree-level diagrams in the left panel of Fig. 4 corresponding to the 2π -exchange, 1π -contact and pure contact graphs (a), (d) and (f), respectively [40, 41]. The shorter-range terms emerging from diagrams (d) and (f) depend on one unknown LEC each which can be determined from suitable few-nucleon observables, see e.g. [6, 5, 38, 39] and references therein. The long-range contribution (a) is driven by the sub-leading $\pi\pi NN$ vertices proportional to the LECs $c_{1,3,4}$ which are known from πN scattering. The

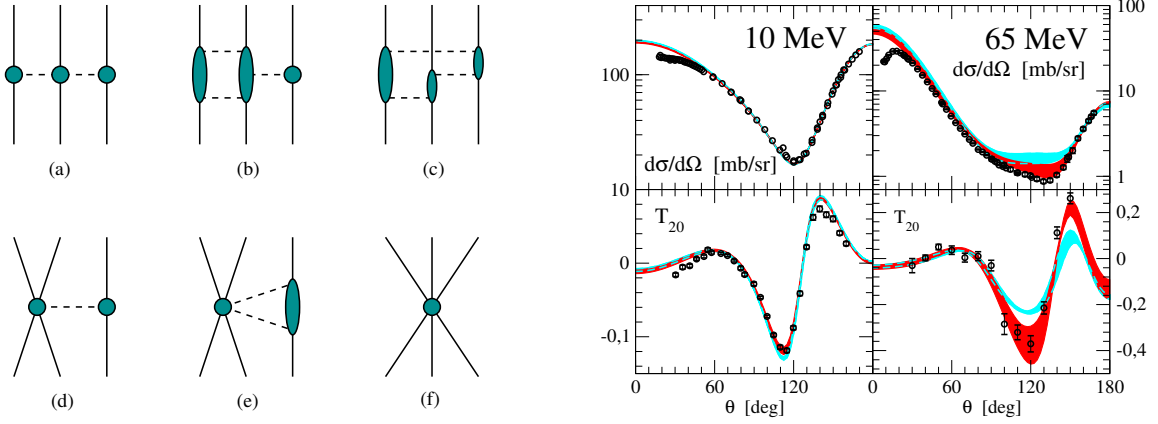


Figure 4: Left panel: Various topologies contributing to the 3NF up to and including $N^4\text{LO}$. Solid and dashed lines represent nucleons and pions while shaded blobs denote the corresponding amplitudes. Right panel: Differential cross section and tensor analyzing power T_{20} for elastic Nd scattering at $E_{\text{lab}}^N = 10$ and 65 MeV. Cyan and red shaded bands correspond to NLO and $N^2\text{LO}$, respectively.

resulting 3NF at $N^2\text{LO}$ has been extensively explored in three- and four-nucleon scattering calculations, see [38] and references therein. One finds a good description of low-energy Nd scattering observables, see Fig. 4 for representative examples, except for the well-known, long-standing puzzles such as the vector analyzing power in elastic Nd scattering (the so-called A_y -puzzle) and the cross section in the space-star breakup configuration, see Ref. [38] for more details. Promising results for low-energy four-nucleon scattering observables based on the chiral 3NF, especially in connection with the A_y -puzzle, are reported in Ref. [42]. While Nd scattering data at higher energies are also well described, the theoretical uncertainty increases rapidly reflecting a similar pattern in the NN sector at this order in the chiral expansion. This is visualized in the right panel of Fig. 4.

Interesting results based on chiral nuclear forces were also obtained by various groups in nuclear structure calculations showing, in particular, sensitivity to the individual terms of the $N^2\text{LO}$ 3NF, see [39] for a review. All these findings clearly underline the need to include corrections to the 3NF beyond the leading terms at $N^2\text{LO}$.

2.3 Open challenges and ongoing work

2.3.1 Renormalization of the NN scattering amplitude with non-perturbative pions

While the long-range part of the nuclear force obeys the standard chiral power counting, the relative importance of the short-range operators and the closely related issue of renormalization of the Lippmann-Schwinger (LS) equation are still under debate, see [43, 44, 45] and references therein for a sample of different points of view. The main problem is due to the fact that iterations of the truncated NN potential within the LS equation generate contributions to the amplitude beyond the order one is working at. These higher-order terms generally involve ultraviolet (UV) divergences which cannot be absorbed by counter terms (contact interactions) included in the truncated potential so that one needs to employ a finite UV cutoff Λ of the order of a natural hard scale, say $\Lambda \sim \Lambda_\chi \sim M_\rho$ [46]. All calculations described in the previous sections have been carried out within such an approach. Notice that it is *not* legitimate to employ $\Lambda \gg M_\rho$ (even if the limit $\Lambda \rightarrow \infty$

of the amplitude exists) unless *all* UV divergences appearing in the iterations of the LS equation are subtracted [47], see Ref. [48] for an illustration. While subleading and higher-order corrections to the potential do not *have to* be resummed in Weinberg's power counting scheme [2] and can be treated perturbatively, it is easy to see that already the LS equation for the LO NN potential

$$V_{2N}^{(0)} = -\frac{g_A^2}{4F_\pi^2} \tau_1 \cdot \tau_2 \frac{\vec{\sigma}_1 \cdot \vec{q} \vec{\sigma}_2 \cdot \vec{q}}{\vec{q}^2 + M_\pi^2} + C_S + C_T \vec{\sigma}_1 \cdot \vec{\sigma}_2, \quad (2.3)$$

where $\vec{\sigma}_i$ (τ_i) denote the Pauli spin (isospin) matrices of a nucleon i and $\vec{q} = \vec{p}' - \vec{p}$ the nucleon momentum transfer, is not renormalizable (in the above-mentioned sense). In [13] we have shown that this unpleasant feature is caused by the nonrelativistic expansion of the NN propagator adopted in the LS equation. We have suggested a new framework based on the manifestly Lorentz invariant effective Lagrangian. In this approach the LO amplitude is obtained by solving the integral equation (first introduced in Ref. [49])

$$T(\vec{p}', \vec{p}) = V_{2N}^{(0)}(\vec{p}', \vec{p}) - \frac{m_N^2}{2} \int \frac{d^3k}{(2\pi)^3} \frac{V_{2N}^{(0)}(\vec{p}', \vec{k}) T(\vec{k}, \vec{p})}{(k^2 + m_N^2)(E - \sqrt{k^2 + m_N^2} + i\epsilon)}, \quad (2.4)$$

where $E = \sqrt{p^2 + m_N^2}$ denotes the center-of-mass energy of a single nucleon. Iterations of this equation generate only logarithmic divergences which can be absorbed into a redefinition of C_S and C_T , i.e. it is perturbatively renormalizable. Consequently, the UV cutoff Λ can be safely removed by taking the limit $\Lambda \rightarrow \infty$. Partial wave projected equations corresponding to Eq. (2.4) have unique solutions except for the 3P_0 channel. The non-uniqueness of the solution in this partial wave can be dealt with by resumming the corresponding counter term, see [13] for more details. We further emphasize that the nucleon mass appearing in the integrand in Eq. (2.4) does not violate the power counting after renormalization is carried out [13, 29]. We already applied this novel scheme to NN scattering at LO. The resulting cutoff-independent phase shifts and mixing angles are shown in Fig. 2. Given that the calculations are carried out at LO, the agreement with the Nijmegen PWA is rather good.

Since we do not rely on the nonrelativistic expansion and do not attempt to integrate out the momentum scale $\sqrt{M_\pi m_N}$, our new scheme can be straightforwardly applied to study the m_q (M_π) dependence of nuclear observables. At LO this is entirely driven by the explicit M_π -dependence of the 1π -exchange potential in Eq. (2.3). Fig. 3 shows the predicted chiral extrapolations of E_{2H} , a_{1S0}^{-1} and a_{3S1}^{-1} . It is comforting to see a good agreement with the N²LO calculations of Ref. [28] based on the formulation with a finite cutoff, see section 2.1.

In the future, these calculations should be extended to higher orders by perturbatively including corrections to the potential. Recent studies [50, 51] within the nonrelativistic framework indicate that such a perturbative treatment of the 2π -exchange might be phenomenologically successful.

2.3.2 Three-nucleon force beyond N²LO

The first corrections to the 3NF emerge at N³LO from all possible one-loop diagrams of type (a)-(e) in Fig. 4 constructed from solely the LO vertices. The resulting parameter-free expressions can be found in Refs. [52, 53], see also Ref. [54]. An interesting feature of the N³LO 3NF corrections is their rather rich isospin-spin-momentum structure emerging primarily from the ring

topology (c) in Fig. 4. This is in contrast with the quite restricted operator structure of the N²LO 3NF. The new structures in the 3NF might have impact on Nd scattering observables and shed light on the existing puzzles. Numerical implementation of the N³LO 3NF corrections requires their partial wave decomposition (PWD) which is a nontrivial task. In Ref. [55], a new method to perform the PWD of any type of the 3NF by carrying out five-dimensional angular integrations numerically was introduced. The PWD of the N³LO 3NF using this new technique requires substantial computational resources and is in progress, see Ref. [56] for some first (but still incomplete) results.

Meanwhile, one may ask whether the chiral expansion of the 3NF is already converged at N³LO. Given the situation with the 2 π -exchange NN potential, where the strongest contributions driven by Δ excitations appear at the subleading order (in that case N²LO), one may expect a similar convergence pattern for the 3NF. This applies especially to new operator structures emerging from the genuine loop topologies (b) and (c), whose chiral expansion starts at N³LO rather than N²LO. At this order, the resulting contributions completely miss effects associated with intermediate $\Delta(1232)$ excitations. To clarify the situation it is, therefore, necessary to go to the next-higher order N⁴LO which corresponds for connected 3N diagrams to the subleading one-loop order. First steps along these lines were made recently in Ref. [57], where the chiral expansion of the longest-range, 2 π exchange 3NF topology was extended to N⁴LO. In the isospin and static limits, the 2 π exchange 3NF in momentum space has the form

$$V_{3N}^{2\pi} = \frac{\vec{\sigma}_1 \cdot \vec{q}_1 \vec{\sigma}_3 \cdot \vec{q}_3}{[q_1^2 + M_\pi^2][q_3^2 + M_\pi^2]} \left(\tau_1 \cdot \tau_3 \mathcal{A}(q_2) + \tau_1 \times \tau_3 \cdot \tau_2 \vec{q}_1 \times \vec{q}_3 \cdot \vec{\sigma}_2 \mathcal{B}(q_2) \right) + 5 \text{ perm.} \quad (2.5)$$

The quantities $\mathcal{A}(q_2)$ and $\mathcal{B}(q_2)$ are scalar functions whose explicit form is computed within the chiral expansion. Notice that the leading nonvanishing contributions to \mathcal{A} and \mathcal{B} at N²LO are governed by the LECs c_i and already take into account effects of the Δ isobar, see the discussion in section 2.2. One may therefore expect a good convergence of the chiral expansion for these quantities. At the N⁴LO (Q^5) level, the functions \mathcal{A} and \mathcal{B} depend on certain combinations of LECs from the order- Q^2 , Q^3 and Q^4 effective πN Lagrangian. Their values were determined in Ref. [57] from πN scattering calculated within the same power counting scheme up to the subleading one-loop order. One then indeed observes a good convergence of the chiral expansion for \mathcal{A} and \mathcal{B} , see the left panel of Fig. 5, which is fully in line with the qualitative arguments given above.

The situation with the intermediate-range contributions emerging from the 2 π - 1 π and ring diagrams (b) and (c) in Fig. 2.2 is completely different. Here, effects of the Δ -isobar start showing up at N⁴LO leading to large corrections at this order [58]. It is more natural to address the convergence of the chiral expansion for long-range 3N potentials in coordinate space. The general structure of a local 3NF in coordinate space can be parameterized in terms of 22 scalar functions $\mathcal{F}_i(r_{12}, r_{23}, r_{31})$ [58]

$$V_{3N} = \sum_{i=1}^{22} \mathcal{G}_i(\vec{\sigma}_1, \vec{\sigma}_2, \vec{\sigma}_3, \tau_1, \tau_2, \tau_3, \hat{r}_{12}, \hat{r}_{23}) \mathcal{F}_i(r_{12}, r_{23}, r_{31}) + 5 \text{ permutations}, \quad (2.6)$$

where $\hat{r}_{ij} \equiv \vec{r}_{ij}/|\vec{r}_{ij}|$ and $\vec{r}_{ij} = \vec{r}_i - \vec{r}_j$ denotes the position of nucleon i with respect to nucleon j . The explicit form of the 22 linearly independent operators \mathcal{G}_i can be found in Ref. [58]. The profile functions \mathcal{F}_i have dimension of energy and can be interpreted as the potential energy between

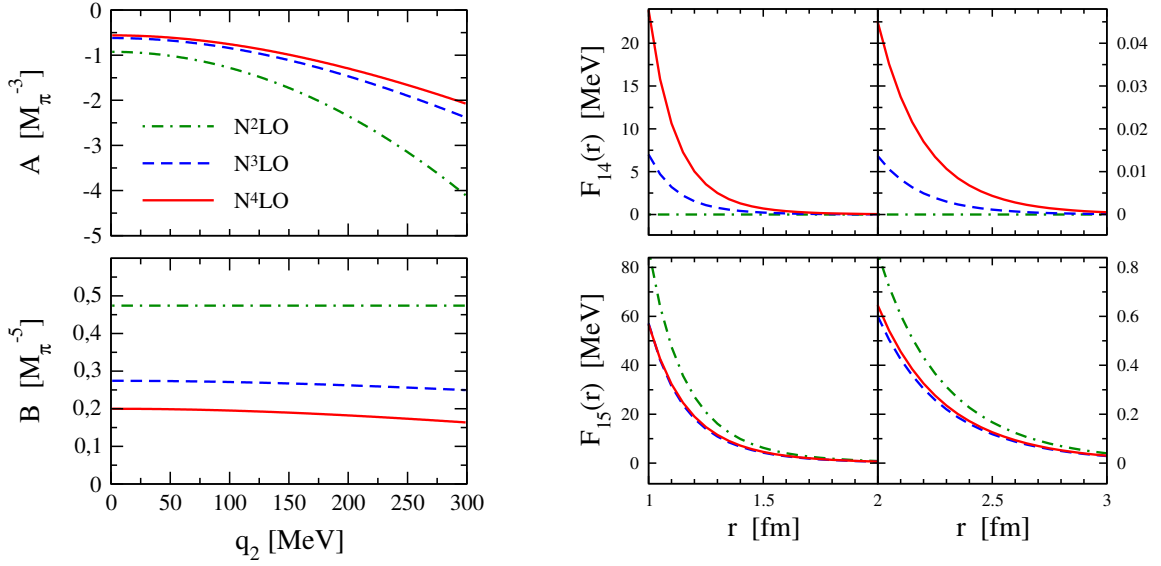


Figure 5: Left panel: Chiral expansion of the functions $\mathcal{A}(q_2)$ and $\mathcal{B}(q_2)$ entering the 2π -exchange 3NF. Right panel: Chiral expansion of the functions $\mathcal{F}_i(r)$ generated by the long- and intermediate-range 3NF topologies up to N⁴LO. Dashed-dotted, dashed and solid lines correspond to $\mathcal{F}_i^{(3)}$, $\mathcal{F}_i^{(3)} + \mathcal{F}_i^{(4)}$ and $\mathcal{F}_i^{(3)} + \mathcal{F}_i^{(4)} + \mathcal{F}_i^{(5)}$, respectively.

three static nucleons projected onto the corresponding operator. They receive contributions from the long-range and intermediate-range 3NF topologies and are predicted (at long distances) by ChPT. This is visualized in the right panel of Fig. 5, where we show the functions \mathcal{F}_{14} and \mathcal{F}_{15} , which accompany the operators $\mathcal{G}_{14} = \tau_2 \cdot \tau_3 \hat{r}_{12} \cdot \vec{\sigma}_1 \hat{r}_{12} \cdot \vec{\sigma}_2$ and $\mathcal{G}_{15} = \tau_1 \cdot \tau_3 \hat{r}_{13} \cdot \vec{\sigma}_1 \hat{r}_{13} \cdot \vec{\sigma}_3$, in the equilateral triangle configuration with $r_{12} = r_{23} = r_{31} = r$. The Fourier transform of Eq. (2.5) corresponding to the longest-range, 2π topology gives rise to 10 out of 22 functions \mathcal{F}_i . They strongly dominate over the intermediate-range contributions at distances $r \gtrsim 2$ fm, so that the chiral expansion of the resulting \mathcal{F}_i 's shows good convergence. The function \mathcal{F}_{15} in Fig. 5 may serve as a representative example. On the other hand, those functions \mathcal{F}_i which do not receive contributions from 2π -diagrams such as e.g. \mathcal{F}_{14} are dominated by the large N⁴LO corrections to the 2π - 1π and ring graphs. Notice that in agreement with the power counting, see Eq. (2.1), 3N potentials are considerably weaker than the NN ones, cf. Fig. 1 and the right panel of Fig. 5. More work is needed to clarify whether phenomenologically important effects associated with intermediate Δ -excitations are already properly represented at N⁴LO. This can be naturally addressed within the Δ -full formulation of χ EFT. Work along these lines is in progress. Last but not least, we emphasize that subleading contributions to the 3N contact interactions (diagram (f) in Fig. 4), which also appear at N⁴LO, are worked out in Ref. [59].

3. Precision few-nucleon physics: Recent examples

Parallel to the developments in the strong sector, there have been several recent applications of χ EFT to few-nucleon reactions with external probes. Here we briefly discuss a few examples.

The first, classical example deals with low-energy pion-deuteron scattering as a tool to extract

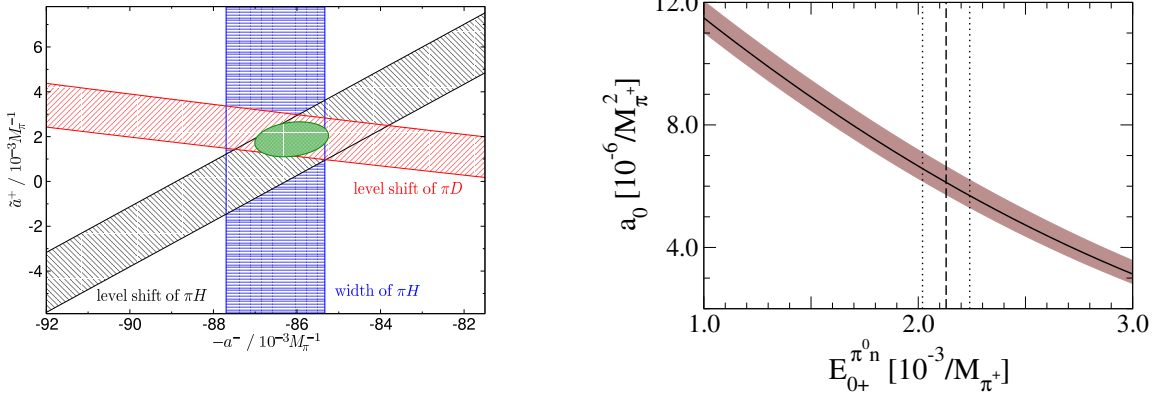


Figure 6: Left panel: Combined constraints on \tilde{a}^+ and a^- from data on πH and πd . Figure courtesy of Vadim Baru. Right panel: sensitivity of a_0 for ${}^3\text{He}$ in units of $10^{-6}/M_{\pi^+}^2$ to the neutron multipole $E_{0+}^{\pi_0 n}$. The vertical dashed line indicates the ChPT prediction for $E_{0+}^{\pi_0 n}$ and the vertical dotted lines the estimated 5% uncertainty. The shaded band gives an indication of the theoretical uncertainty, see [69] for more detail.

the πN isoscalar and isovector scattering lengths a^+ and a^- . Direct extractions of a^+ from πN scattering suffer from large uncertainties, so that the important source of experimental information on these fundamental observables comes nowadays from pionic atoms. Applying an improved Deser formula [60] to the experimentally measured shift and width of the $1s$ level of πH $\varepsilon_{1s} = (-7.120 \pm 0.012)$ eV and $\Gamma_{1s} = (0.823 \pm 0.019)$ eV [61] yields constraints on the scattering lengths shown in Fig. 6. Here, \tilde{a}^+ denotes a particular linear combination of a^+ and isospin-violating terms which is accessible in pionic atoms, see [63] for more details. The πH data alone do not fix even the sign of \tilde{a}^+ . On the other hand, further constraints can be obtained from the recently measured level shift of pionic deuterium [62] πD , $\varepsilon_{1s}^D = (2.356 \pm 0.031)$ eV provided one can reliably relate this observable to πN scattering lengths. Such a theoretical analysis in the framework of χEFT was recently accomplished in [63], see also references therein for earlier calculations. Notice that at this level of accuracy, it was necessary to carefully study isospin-breaking effects. It is comforting to see that the resulting constraints on \tilde{a}^+ and a^- are consistent with those emerging from the πH data. Moreover, combining πH and πD data leads to the best-available determination of \tilde{a}^+ and a^- .

Neutral pion photo- and electroproduction off light nuclei has also been extensively explored in recent years, see Refs. [64, 65] and references therein for earlier studies. Here, one important motivation is to test the ChPT prediction for the neutron amplitude, $E_{0+}^{\pi_0 n} = 2.13 \cdot 10^{-3}/M_{\pi^+}$ [66], which appears to be counterintuitive given the ChPT value for the proton $E_{0+}^{\pi_0 p} = -1.16 \cdot 10^{-3}/M_{\pi^+}$ [66, 67] (which has been confirmed experimentally). While the predicted value for $E_{0+}^{\pi_0 n}$ was verified within 20% by an experiment at SAL using deuteron target [68], it is particularly promising to study π^0 production off ${}^3\text{He}$ which is known to be a good neutron target for spin-dependent observables. Our recent theoretical calculation [69] at subleading one-loop order of χEFT confirms these estimations. It is found that the threshold S-wave cross section for π^0 photoproduction off ${}^3\text{He}$, $a_0 = (|\vec{k}_\gamma|/|\vec{q}_\pi|)(d\sigma/d\Omega)_{\vec{q}_\pi=0}$, is indeed sensitive to the elementary neutron multipole $E_{0+}^{\pi_0 n}$, see the right panel of Fig. 6. Moreover, the uncertainty associated with nuclear corrections appears to be very small so that a reliable theoretical extraction of $E_{0+}^{\pi_0 n}$ from a_0 is possible. Using the

above mentioned ChPT prediction for $E_{0+}^{\pi^0 n}$, the predicted value of the ${}^3\text{He}$ S-wave multipole E_{0+} is roughly consistent with the value deduced from the old Saclay measurement of [70].

There is also considerable interest in electromagnetic few-nucleon reactions. In the single-photon approximation, their theoretical description requires knowledge of the electromagnetic current operator, which should be constructed consistently with the nuclear forces. The derivation of the exchange currents in χEFT was first addressed in the seminal paper by Park et al., [71], who, however, limited themselves to threshold kinematics. Recently, this work was extended by the JLab-Pisa [72] and Bochum-Bonn groups [73] to derive the exchange currents at the one-loop level for general kinematics suitable to study e.g. electron scattering off light nuclei at momentum transfer of the order of $\sim M_\pi$. I do not discuss this topic any further due to the lack of space but refer the reader to Refs. [74] and [75] for recent applications to the magnetic form factor of the deuteron and magnetic moments of light nuclei. Finally, progress in the χEFT treatment of Compton scattering off light nuclei is summarized in Ref. [76].

4. Effective field theory on the lattice

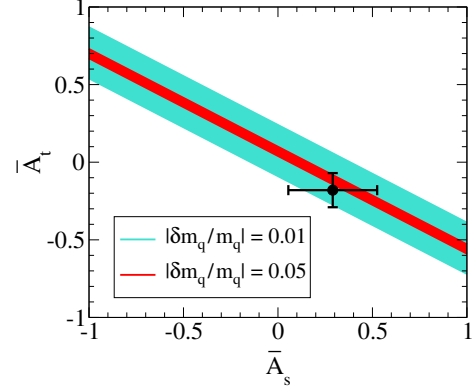
Recently, a *discretized* version of χEFT has been developed and successively applied to compute the properties of few- and many-nucleon systems. In this framework, pions and nucleons are treated as point-like particles on an Euclidean space-time lattice, and the path integral is evaluated by Monte Carlo sampling [77, 78, 79, 80]. Using hadronic DOFs allows one to probe large volumes and greater numbers of nucleons as compared to lattice QCD. Clearly, the method is only applicable at low energies where χEFT is expected to converge.

The crucial object to calculate in our nuclear lattice simulations is the correlation function for A nucleons in the Euclidean space-time, $Z_A(t) = \langle \Psi_A | \exp(-tH) | \Psi_A \rangle$, where $|\Psi_A\rangle$ denotes the Slater determinants for A free nucleons, H is the Hamiltonian of the system and t the Euclidean time. The correlation function can be most efficiently calculated using the Hubbard-Stratonovich transformation to get rid of terms in the action quartic in the nucleon fields (at the expense of introducing interactions with auxiliary fields) and employing the hybrid Monte Carlo technique, see [80] for more details. Once $Z_A(t)$ is computed, the ground state energy of the A -nucleon system can be extracted from the asymptotic behavior of the correlation function for large t , $E_A^0 = -\lim_{t \rightarrow \infty} d(\ln Z_A)/dt$. In a similar way one can also obtain energies of low-lying excited states and compute expectation values of normal ordered operators.

The most advanced studies within this framework are so far performed at N²LO in the chiral expansion. The simulations are carried out using an (improved) LO action which incorporates the physics of the 1π -exchange and the LO NN contact interactions. Higher-order corrections to the nuclear forces including the Coulomb interaction and 3NFs are taken into account perturbatively, see [81] for details. The resulting framework was recently applied to calculate the ground state energies of ${}^4\text{He}$, ${}^8\text{Be}$ and ${}^{12}\text{C}$ as well as the low-lying excitation energies in ${}^{12}\text{C}$ including the the second spin-0 state, the famous Hoyle state [82, 83], see Fig. 7. All calculated energies are in a very good agreement with experiment. While the ground and spin-2 states of ${}^{12}\text{C}$ have been also calculated by other groups using different methods, the results for the Hoyle state are the first *ab initio* calculations. The Hoyle state is known to play a crucial role for producing ${}^{12}\text{C}$, ${}^{16}\text{O}$ and other elements necessary for life via the triple-alpha process in the red giant phase of stars.

	0_1^+	$2_1^+(E^+)$	0_2^+	$2_2^+(E^+)$
LO	-96(2)	-94(2)	-89(2)	-88(2)
NLO	-77(3)	-74(3)	-72(3)	-70(3)
NNLO	-92(3)	-89(3)	-85(3)	-83(3)
Exp	-92.16	-87.72	-84.51	-82(1)

Figure 7: Left panel: Lattice results of Ref. [83] for the energies of low-lying even-parity states of ^{12}C compared to experimental values (in units of MeV). Right panel: “Survivability bands” of carbon-oxygen based life obtained from lattice simulations of Ref. [84] as explained in the text.



The crucial quantity that controls the production rate is the energy ε of the Hoyle state relative to the triple-alpha threshold which is experimentally known to be $\varepsilon = 397.47(18)$ keV. Changing ε by an amount of ± 100 keV results in a strong reduction of the formation of ^{12}C and ^{16}O in the universe making the emergence of carbon-based life impossible. It is, therefore, very interesting to investigate how this seemingly fine-tuned quantity depends on the fundamental constants of nature such as m_q . We have studied the sensitivity of ε to variations of m_q within nuclear lattice simulations in Ref. [84]. Fig. 7 shows the survivability bands of carbon-based life under 1% and 5% changes of m_q . Here, $\bar{A}_{s,t} \equiv (\partial a_{1S0,3S1}^{-1} / \partial M_\pi)_{M_\pi^{\text{phys}}}$ denote the slope of the inverse NN S-wave scattering lengths as functions of the pion mass. These quantities can, in principle, be computed in lattice-QCD. The data point in the right panel of Fig. 7 corresponds to the recent N²LO results of Ref. [28] for chiral extrapolations of $a_{1S0,3S1}^{-1}$ shown in Fig. 3. These findings suggest that the formation of carbon and oxygen in our universe would survive a $\sim 2\%$ change in the light quark mass.

References

- [1] W. Detmold, these proceedings.
- [2] S. Weinberg, Phys. Lett. B **251**, 288 (1990); Nucl. Phys. B **363**, 3 (1991).
- [3] H.-W. Hammer and L. Platter, Ann. Rev. Nucl. Part. Sci. **60**, 207 (2010).
- [4] V. Bernard, Prog. Part. Nucl. Phys. **60**, 82 (2008).
- [5] E. Epelbaum and U.-G. Meißner, Ann. Rev. Nucl. Part. Sci. **62**, 159 (2012).
- [6] E. Epelbaum, H. -W. Hammer and U.-G. Meißner, Rev. Mod. Phys. **81**, 1773 (2009).
- [7] R. Machleidt and D. R. Entem, Phys. Rept. **503**, 1 (2011).
- [8] C. Ordonez, L. Ray and U. van Kolck, Phys. Rev. Lett. **72**, 1982 (1994).
- [9] D. R. Entem and R. Machleidt, Phys. Rev. C **68**, 041001 (2003).
- [10] E. Epelbaum, W. Glöckle and U.-G. Meißner, Nucl. Phys. A **747**, 362 (2005).
- [11] V. G. J. Stoks, R. A. M. Kompl, M. C. M. Rentmeester and J. J. de Swart, Phys. Rev. C **48**, 792 (1993).
- [12] N. A. Arndt *et al.*, SAID online program, <http://gwdac.phys.gwu.edu>.
- [13] E. Epelbaum and J. Gegelia, Phys. Lett. B **716**, 338 (2012).

- [14] M. C. M. Rentmeester, R. G. E. Timmermans and J. J. de Swart, Phys. Rev. C **67**, 044001 (2003).
- [15] M. C. Birse and J. A. McGovern, Phys. Rev. C **70**, 054002 (2004).
- [16] N. Kaiser, S. Gerstendorfer and W. Weise, Nucl. Phys. A **637**, 395 (1998).
- [17] H. Krebs, E. Epelbaum and U.-G. Meißner, Eur. Phys. J. A **32**, 127 (2007).
- [18] V. Bernard, N. Kaiser and U.-G. Meißner, Nucl. Phys. A **615**, 483 (1997).
- [19] T. R. Hemmert, B. R. Holstein, J. Kambor, J. Phys. G **G24** (1998) 1831.
- [20] V. Pascalutsa and D. R. Phillips, Phys. Rev. C **67**, 055202 (2003).
- [21] P. F. Bedaque, T. Luu and L. Platter, Phys. Rev. C **83**, 045803 (2011).
- [22] E. Epelbaum, U.-G. Meißner and W. Glöckle, Nucl. Phys. A **714**, 535 (2003).
- [23] S. R. Beane and M. J. Savage, Nucl. Phys. A **717**, 91 (2003).
- [24] D. B. Kaplan, M. J. Savage and M. B. Wise, Nucl. Phys. B **534**, 329 (1998).
- [25] J. -W. Chen, T. -K. Lee, C. -P. Liu and Y. -S. Liu, Phys. Rev. C **86**, 054001 (2012).
- [26] J. Soto and J. Tarrus, Phys. Rev. C **85**, 044001 (2012).
- [27] J. Mondejar and J. Soto, Eur. Phys. J. A **32**, 77 (2007).
- [28] J. C. Berengut *et al.*, arXiv:1301.1738 [nucl-th].
- [29] E. Epelbaum and J. Gegelia, arXiv:1301.6134 [nucl-th].
- [30] E. Epelbaum, U.-G. Meißner, W. Glöckle and C. Elster, Phys. Rev. C **65**, 044001 (2002).
- [31] E. Epelbaum, Prog. Part. Nucl. Phys. **57**, 654 (2006).
- [32] V. V. Flambaum and R. B. Wiringa, Phys. Rev. C **76**, 054002 (2007).
- [33] S. R. Beane *et al.* [NPLQCD Collaboration], Phys. Rev. D **81**, 054505 (2010).
- [34] M. Albaladejo and J. A. Oller, Phys. Rev. C **84**, 054009 (2011); Phys. Rev. C **86**, 034005 (2012).
- [35] A. M. Gasparyan, M. F. M. Lutz and E. Epelbaum, arXiv:1212.3057 [nucl-th].
- [36] A. Gasparyan and M. F. M. Lutz, Nucl. Phys. A **848**, 126 (2010).
- [37] I. V. Danilkin, A. M. Gasparyan and M. F. M. Lutz, Phys. Lett. B **697**, 147 (2011).
- [38] N. Kalantar-Nayestanaki *et al.*, Rept. Prog. Phys. **75**, 016301 (2012).
- [39] H.-W. Hammer, A. Nogga and A. Schwenk, arXiv:1210.4273 [nucl-th].
- [40] U. van Kolck, Phys. Rev. C **49**, 2932 (1994).
- [41] E. Epelbaum *et al.*, Phys. Rev. C **66**, 064001 (2002).
- [42] M. Viviani, L. Girlanda, A. Kievsky, L. E. Marcucci and S. Rosati, EPJ Web Conf. **3**, 05011 (2010).
- [43] A. Nogga, R. G. E. Timmermans and U. van Kolck, Phys. Rev. C **72**, 054006 (2005).
- [44] M. Pavon Valderrama and E. Ruiz Arriola, Phys. Rev. C **74**, 054001 (2006).
- [45] E. Epelbaum and U.-G. Meißner, nucl-th/0609037.
- [46] G. P. Lepage, nucl-th/9706029.
- [47] E. Epelbaum and J. Gegelia, Eur. Phys. J. A **41**, 341 (2009).

- [48] C. Zeoli, R. Machleidt and D. R. Entem, arXiv:1208.2657 [nucl-th].
- [49] V. G. Kadyshevsky, Nucl. Phys. B **6**, 125 (1968).
- [50] M. Pavon Valderrama, Phys. Rev. C **84**, 064002 (2011).
- [51] B. Long and C. J. Yang, Phys. Rev. C **85**, 034002 (2012).
- [52] V. Bernard, E. Epelbaum, H. Krebs and U.-G. Meißner, Phys. Rev. C **77**, 064004 (2008).
- [53] V. Bernard, E. Epelbaum, H. Krebs and U.-G. Meißner, Phys. Rev. C **84**, 054001 (2011).
- [54] S. Ishikawa and M. R. Robilotta, Phys. Rev. C **76**, 014006 (2007).
- [55] J. Golak *et al.*, Eur. Phys. J. A **43**, 241 (2010).
- [56] R. Skibinski *et al.*, Phys. Rev. C **84**, 054005 (2011).
- [57] H. Krebs, A. Gasparyan and E. Epelbaum, Phys. Rev. C **85**, 054006 (2012).
- [58] H. Krebs, A. Gasparyan and E. Epelbaum, [arXiv:1302.2872 [nucl-th]].
- [59] L. Girlanda, A. Kievsky and M. Viviani, Phys. Rev. C **84**, 014001 (2011).
- [60] V. E. Lyubovitskij and A. Rusetsky, Phys. Lett. B **494**, 9 (2000).
- [61] D. Gotta *et al.*, Lect. Notes Phys. **745**, 165 (2008).
- [62] T. Strauch *et al.*, Eur. Phys. J. A **47**, 88 (2011).
- [63] V. Baru *et al.* Phys. Lett. B **694**, 473 (2011); Nucl. Phys. A **872**, 69 (2011).
- [64] S. R. Beane *et al.*, Nucl. Phys. A **618**, 381 (1997).
- [65] H. Krebs, V. Bernard and U.-G. Meißner, Eur. Phys. J. A **22**, 503 (2004).
- [66] V. Bernard, N. Kaiser and U.-G. Meißner, Eur. Phys. J. A **11**, 209 (2001).
- [67] V. Bernard, B. Kubis and U.-G. Meißner, Eur. Phys. J. A **25**, 419 (2005).
- [68] J.C. Bergstrom *et al.*, Phys. Rev. C **58** (1998) 3203.
- [69] M. Lenkewitz *et al.*, Phys. Lett. B **700**, 365 (2011); arXiv:1209.2661 [nucl-th].
- [70] P. Argan *et al.*, Phys. Lett. **206B** (1988) 4 [Erratum-ibid. B **213** (1988) 564].
- [71] T. -S. Park, D. -P. Min and M. Rho, Nucl. Phys. A **596**, 515 (1996).
- [72] S. Pastore *et al.*, Phys. Rev. C **80**, 034004 (2009); Phys. Rev. C **84**, 024001 (2011).
- [73] S. Kölling *et al.* Phys. Rev. C **80**, 045502 (2009); Phys. Rev. C **84**, 054008 (2011).
- [74] S. Kölling, E. Epelbaum and D. R. Phillips, Phys. Rev. C **86**, 047001 (2012).
- [75] S. Pastore, S. C. Pieper, R. Schiavilla and R. B. Wiringa, arXiv:1212.3375 [nucl-th].
- [76] H. W. Griesshammer *et al.*, Prog. Part. Nucl. Phys. **67**, 841 (2012).
- [77] H. M. Muller, S. E. Koonin, R. Seki and U. van Kolck, Phys. Rev. C **61**, 044320 (2000).
- [78] D. Lee, B. Borasoy and T. Schafer, Phys. Rev. C **70**, 014007 (2004).
- [79] B. Borasoy, E. Epelbaum, H. Krebs, D. Lee and U.-G. Meißner, Eur. Phys. J. A **31**, 105 (2007).
- [80] D. Lee, Prog. Part. Nucl. Phys. **63**, 117 (2009).
- [81] E. Epelbaum, H. Krebs, D. Lee and U.-G. Meißner, Eur. Phys. J. A **45**, 335 (2010).
- [82] E. Epelbaum, H. Krebs, D. Lee and U.-G. Meißner, Phys. Rev. Lett. **106**, 192501 (2011).
- [83] E. Epelbaum, H. Krebs, T. A. Lähde, D. Lee and U.-G. Meißner, Phys. Rev. Lett. **109**, 252501 (2012).
- [84] E. Epelbaum, H. Krebs, T. A. Lähde, D. Lee and U.-G. Meißner, arXiv:1212.4181 [nucl-th].